The cubic mesophase of analogous chiral and achiral hydrazine derivatives

P. Goring; S. Diele; S. Fischer; A. Wiegeleben; G. Pelzl; H. Stegemeyer; W. Thyen

PLEASE SCROLL DOWN FOR ARTICLE

The cubic mesophase of analogous chiral and achiral hydrazine derivatives

P. GÖRING, S. DIELE*, S. FISCHER, A. WIEGELEBEN, G. PELZL

Martin-Luther-Universität Halle-Wittenberg, Institut für Physikalische Chemie, Mühlpforte 1, 06108 Halle/Saale, Germany

H. STEGEMEYER and W. THYEN

Universität GH Paderborn, Institut für Physikalische Chemie, Warburger Str. 100, 33098 Paderborn, Germany

The structures of the cubic mesophases of a chiral and an achiral hydrazine derivative have been investigated by means of X-ray diffraction experiments. As seen from the phase diagram of the binary system, both cubic phases are incompletely miscible which can be explained by the different space groups of the cubic lattices. In contrast to the isotropic liquid, the cubic phase of the chiral compound exhibits a considerable optical rotation indicating phase chirality.

1. Introduction

1,2-Bis-(4-*n*-alkyloxybenzoyl) hydrazines [1] belong to one of the first classes of thermotropic liquid crystal materials where for some members of the series cubic mesophases were found. As shown by Demus *et al.* [2], the octyloxy-, nonyloxy- and decyloxy- homologues exhibit both a cubic and a smectic C phase. In contrast to the 3′-nitro (or 3′-cyano)-4′-*n*-alkyloxybiphenyl-4-carboxylic acids [3–5], the smectic C phase is the high temperature phase.

Later, a number of thermotropic liquid crystal cubic phases were reported. The majority of these compounds are carbohydrates (or related substances) [6–10] and polycatenar compounds [11–16], and there are also examples of metallomesogens with cubic mesophases [17, 18, 26].

In this paper we present the results of structure investigations on the cubic phase of the chiral material 1,2-bis-[4-(3,7-dimethyloctyloxybenzoyl)]hydrazine (**2**). The aim of the investigations was to find out a possible similarity between a chiral cubic phase and the well known chiral blue phases [19]. The results are compared with those obtained for the cubic phase of an analogous achiral compound (**1**). Furthermore, the compatibility (miscibility) of both cubic phases was of special interest. For this reason the phase diagram of the binary system was studied by microscopic as well as by X-ray studies. Some results on the full crystal structure analysis of

compound **1** are discussed in relation to the structure of the cubic phase.

2. Experimental
2.1. *Methods*

The phase transitions were studied by polarized light microscopy (Leitz Orthoplan) using a Linkam THM-1000 hot stage and by differential scanning calorimetry (DSC 7, Perkin Elmer). Structural investigations were performed by X-ray methods (Guinier goniometer, small angle camera, Siemens area detector). Monodomains of the cubic phase were obtained by slow cooling from the isotropic phase in the presence of a magnetic field. The wavelength dispersion of the optical rotation was measured using a spectropolarimeter (Jasco 7–20).

2.2. *Materials*
2.2.1. *1,2-Bis-(4-n-octyloxy-benzoyl)hydrazine (1)*

The achiral derivative **1** was prepared as described in [1]. The phase transition temperatures (in °C) are given below together with the molecular structure.

As seen from the transition scheme the achiral compound exhibits a smectic C phase besides the cubic phase. The transition cubic–smectic C is strongly influenced by the heating and cooling rate. The hysteresis of the phase transitions is displayed in figure 1.

At a fast heating rate, the smectic C phase can be suppressed (trace a). If the isotropic liquid is kept sufficiently long well above the clearing temperature, the SmC phase appears on cooling the isotropic liquid

*Author for correspondence.
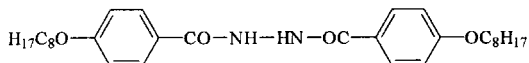
1 $H_{17}C_8O$—[benzene]—CO—NH—HN—OC—[benzene]—OC_8H_{17} Cr1 129·5 Cr2 140·8 Cub 158·4 SmC 162·3 I

Figure 1.   Transition scheme for the achiral compound **1**. The numbers at the transition peaks designate the transition enthalpy in $kJ\,mol^{-1}$.

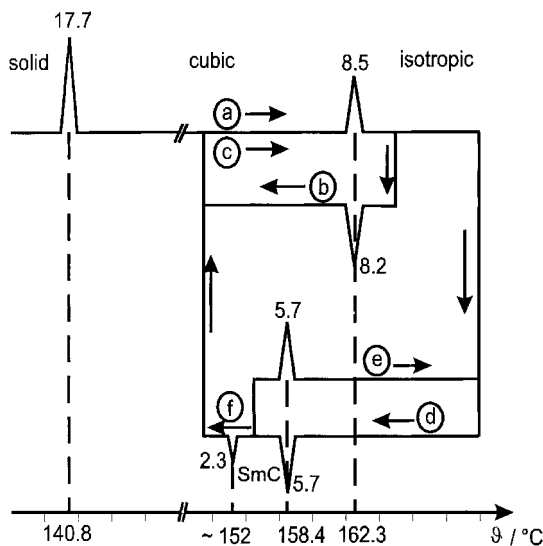(trace d). On the other hand, on cooling the sample immediately after the transition into the isotropic liquid, the smectic C phase could not be observed (trace b). The results have been explained by pretransitional effects [2] or a kinetically determined process. However, with respect to the discussions about lattice melting at the clearing point [27], our results can be explained by the assumption that nuclei of the cubic phase exist above the clearing point, but are destroyed at the higher temperatures which must be reached in order to obtain the SmC phase during the cooling process. But in contrast to [27, 28] a calorimetric effect could not be detected above the clearing temperature.

2.2.2. *1,2-Bis[4-(3,7-dimethyloctyloxybenzoyl)]hydrazine (2)*

The chiral derivative **2** has two chiral centres (*) in the side chains. Starting from (*S*)-(-)-β-citronellol, **2** was synthesized following the route given in the scheme. The overall yield was 10%. **2** was purified by repeated recrystallization from ethanol; optical rotation at 25°C in $CHCl_3$ ($10\,mg\,ml^{-1}$): $-5\cdot2^\circ$ (Na-D).
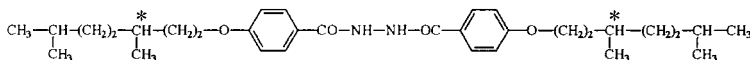
The structure of **2** is given below together with the phase transition temperatures (in °C). The DSC thermogram of **2** is displayed in figure 2.

Compound **2** only exhibits a cubic phase which could be distinguished from the isotropic liquid by polarizing microscopy only by the fact that movement of air bubbles suddenly stopped at the phase transition from the isotropic liquid.

The introduction of the lateral CH_3 groups depresses the clearing temperature in comparison with the achiral compound. On cooling the cubic phase, no crystallization is observed down to room temperature; only after some days does the sample begin to crystallize.

The optical rotation of **2** is shown in figure 3 as a function of the wavelength.

In the isotropic liquid there is only an extremely small signal caused by the molecular optical activity of **2**. However, in the cubic phase (below 135°C), a considerable optical rotation has been found, with a strong increase on decreasing the wavelength. This rotatory dispersion indicates phase chirality. Because of the small lattice constant of the cubic phase (see §3·2) one can presume that an anomalous rotatory dispersion will occur in the far UV as has been found for cubic blue phases in the visible region [20].

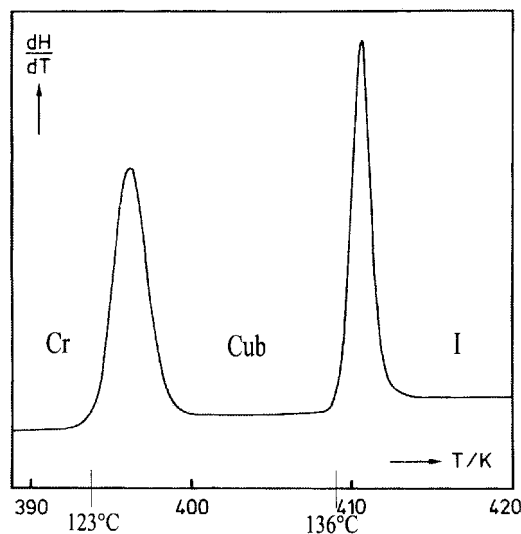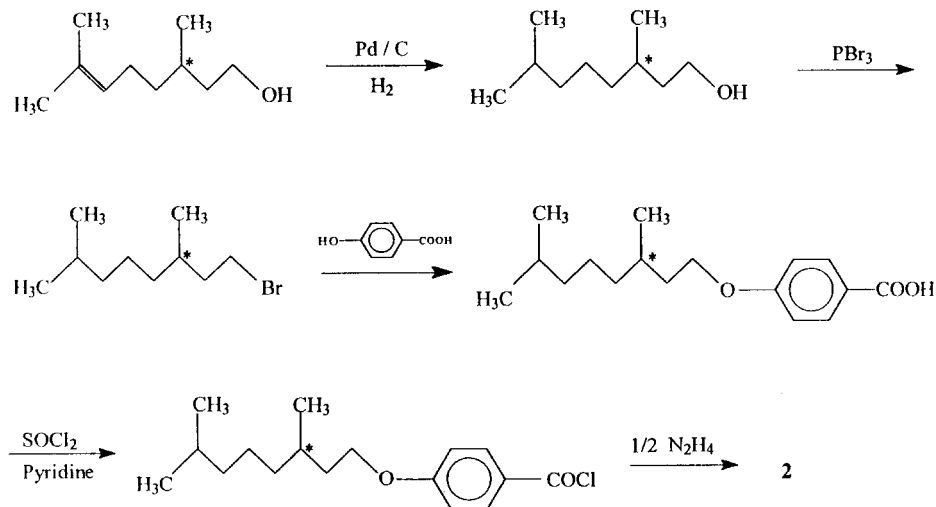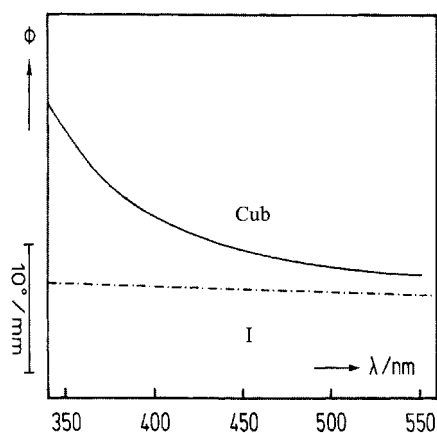Figure 2.   DSC trace for the chiral compound **2** showing the phase transitions Cr–Cub–I.

2 CH_3—CH—$(CH_2)_2$—*CH—$(CH_2)_2$—O—[benzene]—CO—NH—NH—OC—[benzene]—O—$(CH_2)_2$—*CH—$(CH_2)_2$—CH—CH_3 with CH_3 substituents   Cr 124–128 Cub 135·6 I

CH₃ CH₃

H₃C OH —Pd / C, H₂→ CH₃ CH₃ H₃C * OH —PBr₃→

CH₃ CH₃ H₃C * Br —HO—⟨⟩—COOH→ CH₃ CH₃ H₃C * O—⟨⟩—COOH

—SOCl₂ / Pyridine→ CH₃ CH₃ H₃C * O—⟨⟩—COCl —1/2 N₂H₄→ **2**

Scheme 1

Figure 3. Wavelength dispersion of the optical rotation ϕ in the cubic phase (full line) and the isotropic liquid (dashed line) of compound **2**.

3. Results

3.1. *The achiral compound 1*

Single crystals of sufficient quality were obtained, and the results of the full structure analysis will be reported in a separate paper [20]. Compound **1** crystallizes in a triclinic cell with the space group $P1$. The dimensions of the unit cell are $a = 0.4987(7)$ nm, $b = 1.1549(8)$ nm, $c = 1.3466(9)$ nm, $\alpha = 112.23(3)°$, $\beta = 94.27(3)°$ and $\gamma = 95.10(3)°$.

The molecules form sheets linked by hydrogen bonds (see figure 4). The N–H ... O distance is 0.2985 nm. A solid–solid transition at $\vartheta = 129.5°C$ prevents a direct comparison of the molecular packing found by the full structure analysis with that of the cubic phase. The packing of the molecules in the crystalline phase may be considered more as a precursor for a layer structure than for a cubic one.

Figure 5 presents the X-ray diffraction diagram of the cubic and smectic C phases of the achiral compound as registered by a Guinier goniometer. In accordance with earlier measurements [2] we found in the small angle region several reflections (the intensities of which are different by more than two orders of magnitude) and a diffuse scattering at about 10°. The θ values, and the Miller indices are summarized in table 1. But in contrast to [2] the $\sin \theta$ values of these reflections match the proportions $\sqrt{3}: \sqrt{4}: \sqrt{7}: \sqrt{8}: \sqrt{10}$. Since the ratio $\sqrt{7}$ is not compatible with a cubic lattice, the sequence of numbers must be doubled, so that the following ratios result $\sqrt{6}: \sqrt{8}: \sqrt{14}: \sqrt{16}: \sqrt{20}$. From this indexing not only a higher lattice parameter ($a = 6.46$ nm) is calculated compared with that of [2], but also another space group: a body centred cubic cell with the designation $I\bar{4}3d$ or $Ia3d$. Only these space groups of a body centred unit cell can explain the absence of reflections with the lower Miller indices (1 0 0, 1 1 0, etc.).

We were able to investigate the smectic phase above the cubic phase by X-ray investigations of oriented samples. After longer heating above the clearing temperature and cooling the sample below 164°C we obtained the typical scattering diagram of an oriented smectic phase with liquid-like order in the smectic layers [figure 6(a)].

From the relative positions of the maxima of the small angle reflections and those of the diffuse wide angle scattering which have been measured by a χ scan, a tilt angle of about 20° with an error of about $\pm 3°$ can be estimated, which proves the existence of a smectic C phase. Using this angle and the measured d-value of the SmC phase ($d_{SmC} = 2.75$ nm) we can estimate the length l of the building units ($l = d_{SmC}/\cos 20° = 2.9$ nm) of the layer structure. It can be seen that this value strongly
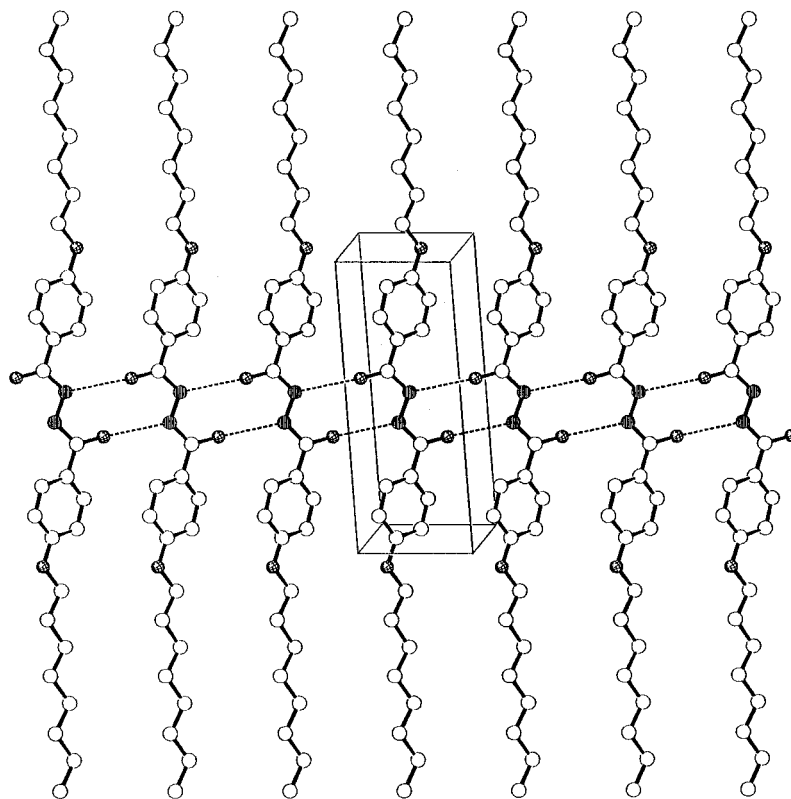
Figure 4. Packing   and   crystal structure of **1**: projection onto (0 3 1).
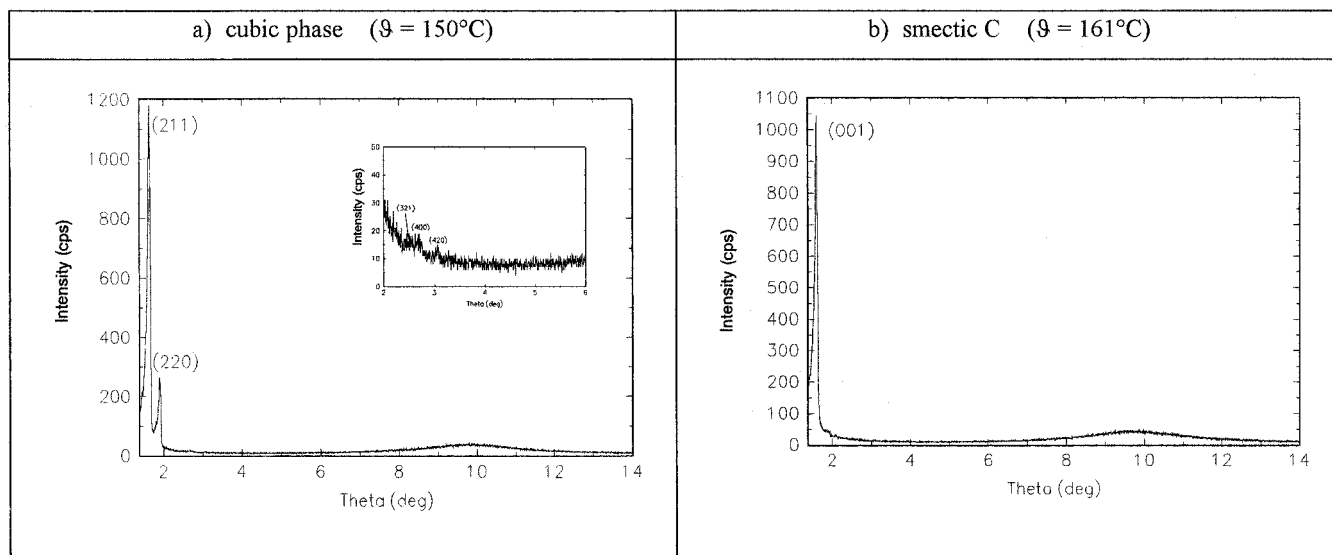

Figure 5.   X-ray diffraction diagram of the cubic phase (150°C) and smectic C phase (161°C) of compound **1** obtained by a Guinier goniometer.

deviates from the length of the molecule ($L = 3 \cdot 78$ nm) which has been measured by the full structure analysis [2]. This points to an essential change of the molecular conformation in the liquid crystalline phase. (An explanation of the difference, L-l = 0·88 nm, by inter-

calation of molecules of neighbouring layers is unlikely for compounds with this chemical structure.)

On cooling down the sample, the (0 0 1) reflection is shifted only very slightly and corresponds now to the (2 1 1) reflection of the cubic phase. The pattern of a

Table 1. Small angle reflections of the cubic phase of compound **1**; θ-values, and the Miller indices $(h\,k\,l)$

$\theta_{exp}/°$	$\theta_{calc}/°$	$(h\,k\,l)$
1·67	—	2 1 1
1·95	1·95	2 2 0
2·58	2·58	3 2 1
2·75	2·76	4 0 0
3·08	3·08	4 2 0

monodomain of the cubic phase is shown in figure 6 (*b*). The indexing sketched in figure 7(*a*) and proved by a computer simulation using the CERIUS program [figure 7(*b*)] leads to the direction of incidence along the axis [0 1 1] or [1 0 1], respectively.

The epitaxial relation between the [0 0 1] planes of the lamellar phase and the {2 1 1} planes of the cubic phase has been discussed extensively for lyotropic sys-

tems [24]. Some metal complexes exhibit a thermotropic SmC phases below the cubic *Ia3d* phase [18], and there too the transition of the [0 0 1] planes into the {2 1 1} planes of the cubic phase has been evidenced. Therefore this kind of epitaxial relation seems to be a specific feature of the transition from a layer structure into a *Ia3d* phase, whereas in the case of a transition into a *Im3m* structure, the relation between the [0 0 1] planes and the {2 2 2} planes has been found [25].

Finally the appearance of a diffuse scattering, figure 6(*b*), between the reflections (1̄21) and (2̄02), (2̄02) and (1̄2̄1), (1̄2̄1) and (20̄2), (20̄2) and (121̄) should be emphasized. This scattering has been explained in [18] and [24] by a displacement of parallel rows in the [1 1 1] direction with respect to each other. On the basis of the structural model given first in [23], a line in the [1 1 1] directions connects the junctions of the rods linked three by three [figure 12(*b*)]. However, it is necessary in the case under consideration to check the
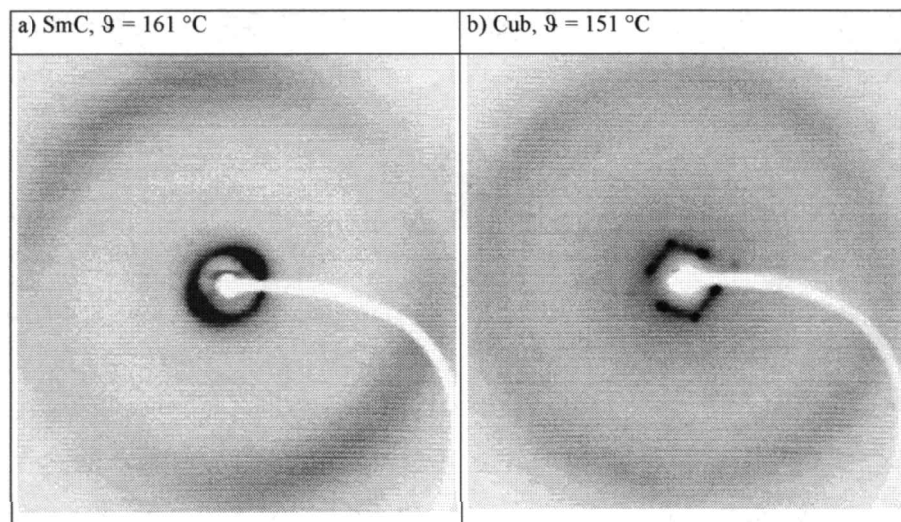

Figure 6. X-ray diffraction pattern of an oriented sample (*a*) of the smectic C phase (161°C) and (*b*) the cubic phase (151°C) of compound **1**.
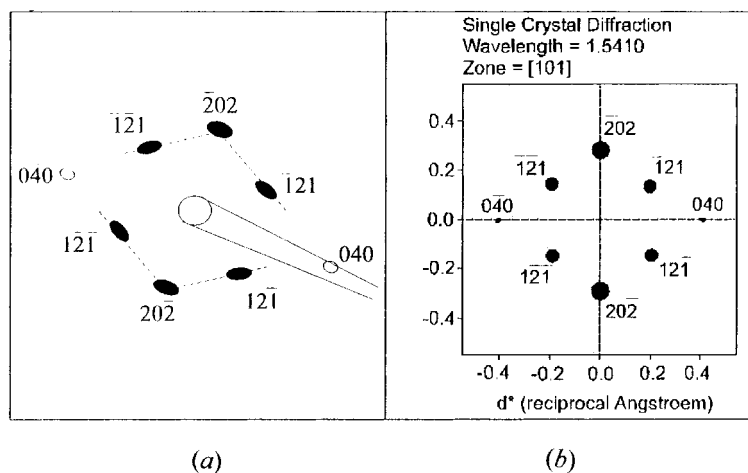

Figure 7. Indexing of the reflections of figure 6 (*b*) (*a*) and the corresponding section of reciprocal plane calculated by the CERIUS program (*b*).
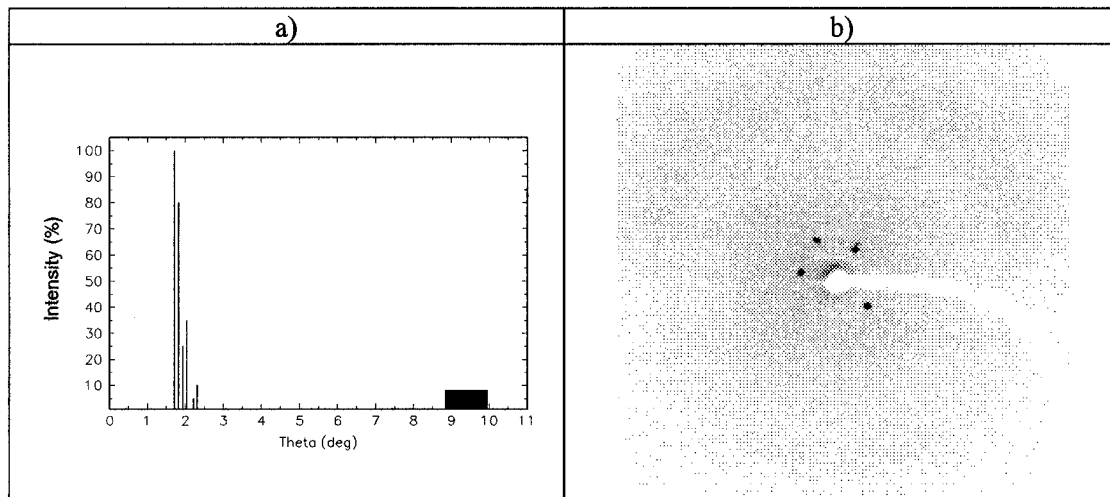
Figure 8. (*a*) Schematic representation of the X-ray reflections of the cubic phase of compound **2**. (*b*) X-ray diffraction pattern of an oriented cubic sample; the lower part of the pattern is shadowed by the heating stage.

direction of the diffuse plane in reciprocal space using different incidence angles of the primary beam.

3.2. *The chiral compound* **2**

Figure 8(*a*) displays schematically the reflections and relative intensities for the cubic mesophase of the chiral compound **2** obtained from the Guinier film pattern. In table 2 the θ-values of the small angle reflections and Miller indices are summarized.

The small number of reflections does not allow us to select a definite space group. The space groups $I23$, $I2_13$, $Im3$, $I432$, $I43m$, $Im3m$ and $I4_132$ are compatible with the observed reflections. But the observed optical activity demands a point group symmetry 23 or 432. Among the listed space groups only the space groups $I23$, $I2_13$, $I432$ and $I4_132$ fulfil the conditions [28]. The indexing under this assumption leads to a lattice parameter of about 9·64 nm.

The pattern of an oriented sample is quite similar to that of the achiral compound with the exception that the diffuse scattering between the Bragg spots does not exist [see figure 8(*b*)].

Table 2. Small angle reflections of the cubic phase of compound **2**; θ-values and Miller indices ($h\,k\,l$)

$\theta_{exp}/°$	$\theta_{calc}/°$	(h k l)
1·71	—	3 2 1
1·83	1·83	4 0 0
1·94	1·94	4 1 1
2·04	2·05	4 2 0
2·22	2·24	4 2 2
2·31	2·33	4 3 1

3.3. *Phase diagram of the binary system*

Since like liquid crystalline phases give complete miscibility [21] over broad composition ranges, this behaviour should be checked for the substances under consideration. The similar chemical structures should favour complete miscibility.

The phase diagram (figure 9) has been checked by DSC and X-ray studies. The X-ray studies show a break in the features of the patterns at around 50 mol% (figure 10). It is remarkable that the gap is very narrow.
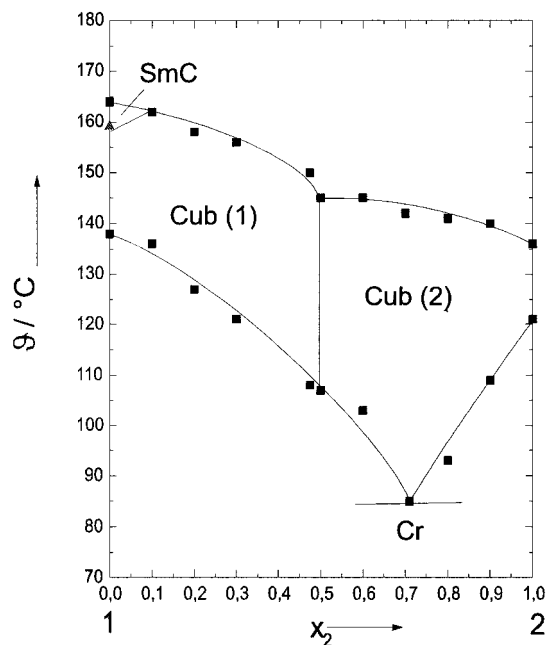

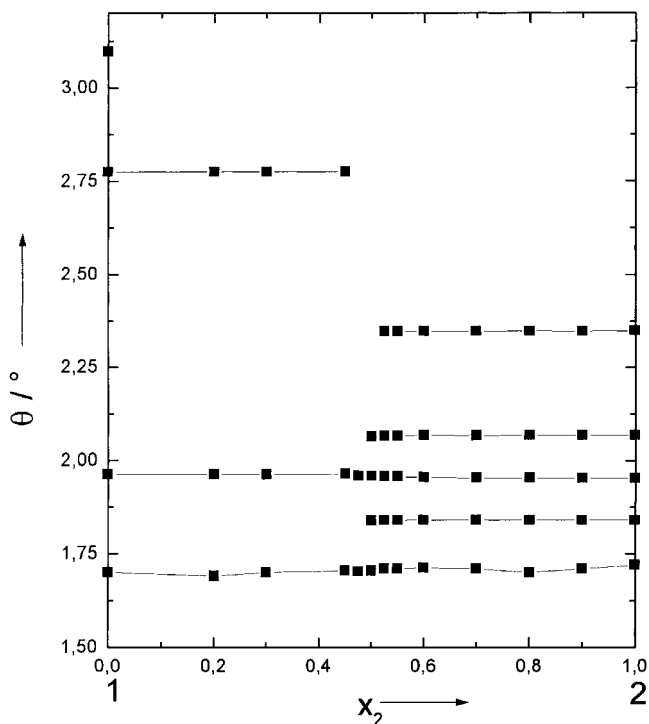Figure 9. Phase diagram for the chiral and achiral hydrazine derivatives.

Figure 10. Small angle reflections in the cubic phases of the binary systems as a function of concentration.

Figure 11. Contact preparation of compound **1** (left) and compound **2** (right) at 132°C. The birefringence on the left is caused by the crystallization of **1**. The borderline between the two cubic phases is marked by arrows.

The concentration at the borderline follows from investigations of the dependence of X-ray characteristics on concentration. As seen from figure 10, up to 50 mol% only the reflections of the achiral hydrazine are observed, and above 50 mol% only reflections of the chiral compound appear. It should be noted that the positions of the reflections remain nearly unchanged in their dependence on concentration and temperature.

As shown in figure 11, the contact preparation photomicrograph proved the miscibility gap between the cubic phases. The cubic phases of the chiral and achiral components are not therefore completely miscible, although their chemical structures are very similar. The same result, caused by the different symmetry of the different space groups has been reported recently in [22].

4. Discussion

It is remarkable that in spite of their quite similar molecular structures, each compound forms a different cubic mesophases; the lattice constant, as well as the space group is clearly different in the two cubic phases. These differences give rise to the immiscibility of the cubic phases as seen from the phase diagram of the binary system. Nevertheless, a considerable amount of chiral component **2** can be incorporated into the lattice
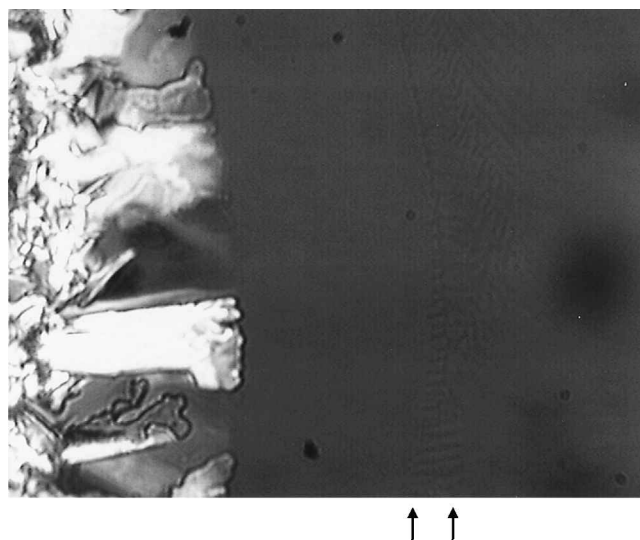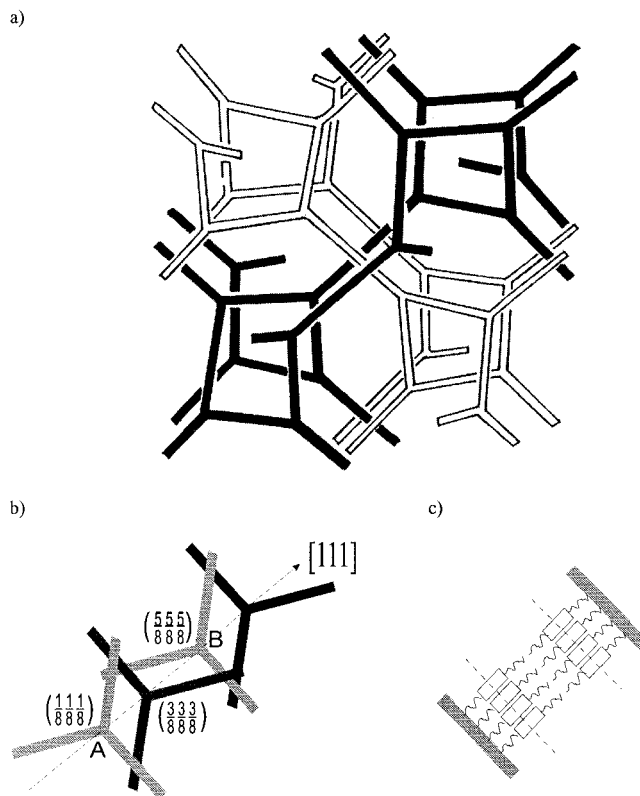

Figure 12. Possible molecular arrangement in the cubic phase.

of achiral compound **1** without changing its space group, and *vice versa*. Obviously at 50 mol% the lattice type suddenly changes.

The question arises as to what are the structural units of these cubic phases. It follows from the structure investigation on the solid crystal that there exist sheets which are obviously linked by hydrogen bonds. It can be assumed that such sheets, stabilized via hydrogen bonds, are the structural units in the cubic structure too. The X-ray data are not sufficient to prove a molecular packing in the cubic phase, but for the *Ia*3*d* space group two interwoven, but unconnected networks of rods linked three by three have been described [18, 23, 24] [figure 12(*a*)]. If the measured parameter *a* of compound **1** is used to calculate the distance between the junctions

$$\left(A = \left(\frac{1}{8} \frac{1}{8} \frac{1}{8} \right) *a, \quad B = \left(\frac{5}{8} \frac{5}{8} \frac{5}{8} \right) *a \right)$$

of one of the two three-dimensional networks [figure 12(*b*)] a value of 5·8 nm is obtained, which agrees very well with twice the apparent length of the molecule in the liquid crystalline phase. This is the distance between the parallel rods in the networks generally, and supposes the idea that the molecules are positioned between the rods of one network in a manner such that the methyl groups of the terminal alkyl chains are located on the rods to form planes [figure 12(*c*)].

Since the planes (spread between the parallel rods of one and the same network) interpenetrate the planes of the second network perpendicularly, the alignment of the molecules at the crossing point can be understood. The location of the molecules around the 3-fold points (which have to fulfil the condition of a 4-fold screw axis), as well as the extension of the assumed sheets into cylindrical rods or fragments of layers, cannot however be answered in this way. In forthcoming studies we will check some models using calculations based on the bicontinuous minimal surface model.

References

[1] SCHUBERT, M., HAUSCHILD, J., DEMUS, D., and HOFFMANN, S., 1978, *Z. Chem.*, **18**, 256.

[2] DEMUS, D., GLOZA, A., HARTUNG, H., HAUSER, A., RAPTHEL, I., and WIEGELEBEN, A., 1981, *Cryst. Res. Technol.*, **16**, 1445.

[3] GRAY, G. W., JONES, B., and MARSON, F., 1957, *J. chem. Soc.*, 395.

[4] PELZL, G., and SACKMANN, H., 1971 *Symp. Faraday Soc.*, **5**, 68.

[5] DIELE, S., BRAND, P., and SACKMANN, H., 1972, *Mol. Cryst. liq. Cryst.*, **17**, 163.

[6] KOHNE, B., PRAEFCKE, K., and BILLARD, J., 1986, *Z. Naturforsch. (b)*, **41**, 1036.

[7] LATTERMANN, G., and STAUFER, G., 1990, *Mol. Cryst. liq. Cryst.*, **191**, 199.

[8] FISCHER, S., FISCHER, H., DIELE, S., PELZL, G., JANKOWSKI, R., SCHMIDT, R. R., and VILL, V., 1994, *Liq. Cryst.*, **17**, 855.

[9] BORISCH, K., DIELE, S., GÖRING, P., MÜLLER, H., and TSCHIERSKE, C., 1997, *Liq. Cryst.*, **22**, 427.

[10] BORISCH, K., DIELE, S., GÖRING, P., and TSCHIERSKE, C., 1997, *Angew. Chem. int. Ed. Engl.*, **36**, 2087.

[11] TINH, N. H., DESTRADE, C., LEVELUT, A. M., and MALTHETE, J., 1986, *J. Phys. Fr.*, **47**, 553.

[12] LEVELUT, A. M., MALTHETE, J., DESTRADE, C., and TINH, N. H., 1987, *Liq. Cryst.*, **2**, 877.

[13] FANG, Y., LEVELUT, A. M., and DESTRADE, C., 1990, *Liq. Cryst.*, **7**, 265.

[14] ALSTERMARK, C., ERIKSSON, N., NILSSON, M., DESTRADE, C., and TINH, N. H. 1990, *Liq. Cryst.*, **8**, 75.

[15] WEISSFLOG, W., LETKO, I., PELZL, G., and DIELE, S., 1995, *Liq. Cryst.*, **18**, 867.

[16] LETKO, I., DIELE, S., PELZL, G., and WEISSFLOG, W., 1995, *Liq. Cryst.*, **19**, 643.

[17] BRUCE, D. W., DUNMUR, D. A., HUDSON, S. A., LALINDE, E., MAITLIS, P. M., McDONALD, M. P., ORR, R., STYRYNG, P., CHERODIAN, A., RICHARDSON, R. M., FEIJOO, J. L., and UNGAR, G., 1991, *Mol. Cryst. liq. Cryst.*, **206**, 79.

[18] BRUCE, D. W., DONNIO, B., HUDSON, S. A., LEVELUT, A. M., MEGTERT, ST., PETERMANN, D., and VEBER, M., 1995, *J. Phys. II Fr.*, **5**, 289.

[19] For reviews of blue phases see: STEGEMEYER, H., BLÜMEL, TH., HILTROP, R., ONUSSEIT, H., and PORSCH, F., 1986, *Liq. Cryst.*, **1**, 3; CROOKER, P. P., 1989, *Liq. Cryst.*, **5**, 751.

[20] THYEN, H., STEGEMEYER, H., FLÖRKE, U., and HAUPT, H.-J., (in preparation).

[21] DEMUS, D., DIELE, S., GRANDE, S., and SACKMANN, H., 1983, *Advances in Liquid Crystals*, Vol. 6 (Academic Press), p. 1.

[22] LEVELUT, A.-M., and CLERC, M., 1998, *Liq. Cryst.*, **24**, 105.

[23] LUZATTI, V., and SPEGT, P. A., 1967, *Nature*, **215**, 701.

[24] RANCON, Y., and CHARVOLIN, J., 1987, *J. Physique*, **48**, 1067.

[25] HENDRIKX, Y., and PANSU, B., 1996, *J. Phys. II Fr.*, **6**, 33.

[26] DONNIO, B., HEINRICH, B., GULIK-KRZYWICKI, T., DELACROIX, H., GUILLON, D., and BRUCE, D. W., 1997, *Chem. Mater.*, **9**, 2951.

[27] GOODBY, J. W., DUNMUR, D. A., and COLLINGS, P. J., 1995, *Liq. Cryst.*, **19**, 703.

[28] KUTSUMIZU, S., YAMADA, M., and YANO, S., 1994, *Liq. Cryst.*, **16**, 1109.

[29] NYE, J. F., 1985, *Physical Properties of Crystals*, Oxford Science Publication (Oxford: Clarendon Press).